

Stability Analysis of Inverter-Based Systems with Virtual Inertia Control

P. S. A. PEIRIS

**Department of ECE, University of Manitoba, Winnipeg, MB,
Canada**

S. FILIZADEH

**Department of ECE, University of Manitoba, Winnipeg, MB,
Canada**

B. JAYASEKARA

**Manitoba Hydro International, Winnipeg, MB,
Canada**

L. KOTHALAWALA

**Manitoba Hydro International, Winnipeg, MB,
Canada**

D. MUTHUMUNI

**Manitoba Hydro International, Winnipeg, MB,
Canada**

SUMMARY

This paper describes model development and stability analysis of a grid-forming inverter-based system with inertia emulation capability. A mathematical model is developed and linearized to obtain a small signal model of a two-inverter, single-load system; eigenvalue analysis is then conducted to analyse the stability aspects of emulating inertia using specialized power control loops. The system's eigenvalues and their trajectories are compared with a small signal model of a grid-forming inverter with only droop controllers (no inertia emulation).

Benchmark EMT models are also developed to compare the response of the small signal model to verify the accuracy of the developed linearized model and its predictions. Eigenvalue sensitivities of the generating units when operating with droop coefficients and inertial parameters are presented.

KEYWORDS

Virtual Inertia, Grid Forming, Stability, Eigenvalue analysis, EMT simulations, Mathematical Modelling.

INTRODUCTION

The escalating penetration of renewable resources has caused a shift from conventional synchronous machine-based generation to inverter-tied generation in many power systems around the world. System inertia, which is commonly provided by the large rotating masses of synchronous generators, is drastically reduced in inverter-tied generation schemes. Reduced inertia has a direct impact on the stable operation of renewable generation plants as well as the overall system stability. Therefore, the industry has identified that it is advantageous to emulate such inertial dynamics in inverter-tied systems using converter control algorithms known as grid-forming methods.

Grid-forming converters can be classified into three main categories: rigid converters where the voltage and frequency is maintained at a fixed setpoint, droop-controlled non-inertial converters where the voltage and frequency are varied in conjunction with active and reactive power, and lastly inertial converters, which have inertia emulation in their power-frequency control loops. Synchronverters [1], virtual oscillators [2], [3], decoupled voltage and current controlled converters [4], and angle droop-based converters [5] are some of the common grid-forming converter schemes.

Small signal modelling and eigenvalue analysis have already been used to study the stability of droop-based converter systems that have decoupled voltage and current control loops [6], [7]. There is, however, a requirement to study the interactions between inertia emulating grid-forming inverters using small signal analysis to identify the impact of converter inertia emulation on system stability.

This paper presents a stability analysis conducted on a two-source, single-load system that includes inertia emulating grid-forming voltage source converters (VSCs). The system with two inertia emulating converters is then compared in the same setup with grid-forming converters that have simple (P- ω and Q-V) droop control and no inertia emulation. The systems are mathematically modelled and linearized to obtain their small signal models. An eigenvalue analysis is conducted, and the sensitive modes and their associated states are identified using participation factors.

The paper proceeds with a description of the system in Section 2. Mathematical modelling is presented in Section 3. Results are presented in Section 4 followed by conclusions in Section 5.

2. DEVELOPMENT OF THE TEST SYSTEM.

A grid-forming converter has a three-stage control topology, which includes an outer power control loop with cascaded voltage and current control loops. The power control stage consists of active and reactive power droop controllers whereas the power-frequency droop controller generates a frequency reference with inertia emulation. The reactive power controller generates a voltage reference using the reactive power measurement of the converter terminals. Figure 1 shows these loops, which generate the frequency and voltage reference for the decoupled voltage and current controllers.

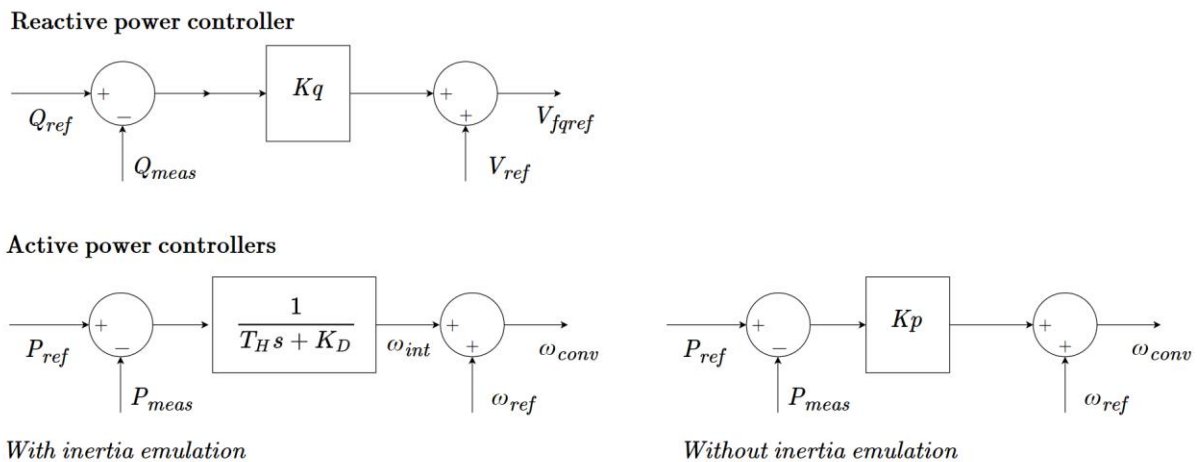


Figure 1. Power-stage controllers.

The reactive power controller can be described using the following expression:

$$V_{qref} = V_{ref} - K_q (Q_{meas} - Q_{ref}) \quad (1)$$

where K_q is the proportional gain of the reactive power loop.

The equation for the active power stage in the inertia emulating converter is as follows.

$$\omega_{conv} = \omega_{ref} + \frac{1}{\left(\frac{T_H s}{K_D} + 1 \right)} (P_{ref} - P_{meas}) \quad (2)$$

Once the transients are settled, the static droop coefficient (K_p) for active power loop becomes $1/K_D$. The equation can be arranged in the form of a swing equation similar to a synchronous machine as follows.

$$T_H \frac{d(\omega_{conv} - \omega_{ref})}{dt} = P_{ref} - P_{meas} - K_D (\omega_{conv} - \omega_{ref}) \quad (3)$$

This gives an inertia constant of $H = (T_H/2)$ and a damping coefficient of $D = K_D$ as analogous to the synchronous machine [8], [9].

The voltage and current controllers consist of a decoupled controller, which generate the voltage reference of the VSC. The voltage controller receives the voltage reference from the reactive power control loop while the frequency reference from the active power loop is utilized to generate the transformation angle of the decoupled control (dq) loop. The outer voltage controllers generate a current reference for an inner current control loop, which is used for current limiting and improved performance. Figure 2 shows the control diagram of voltage and current controllers.

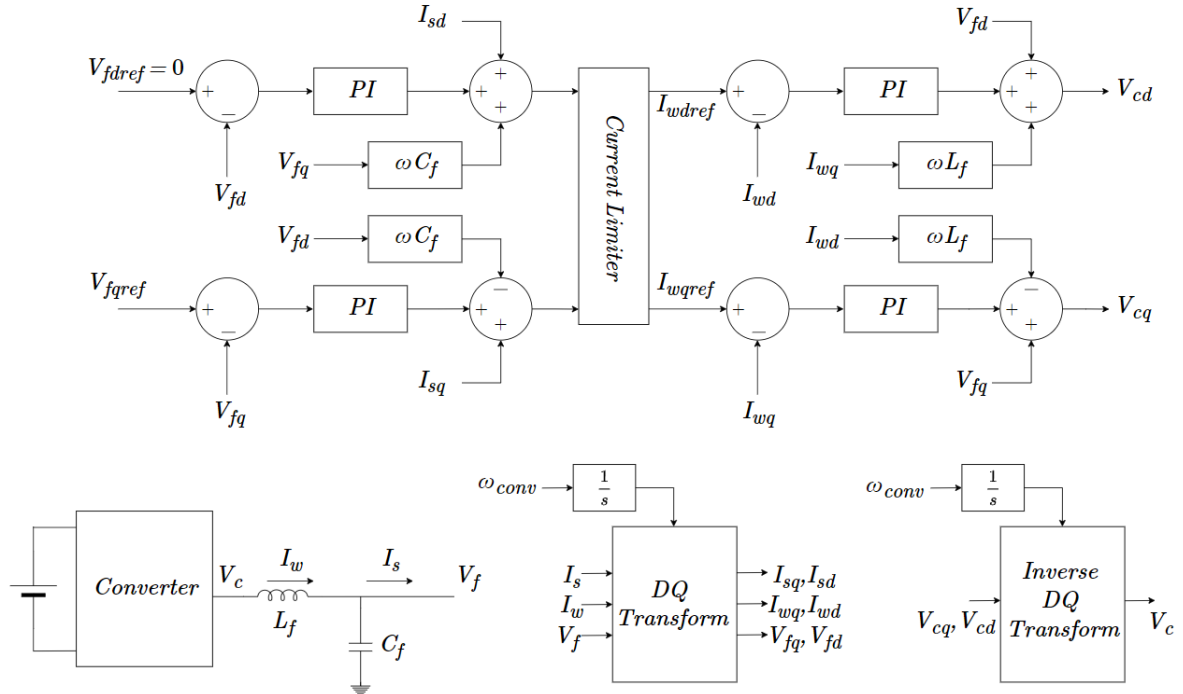


Figure 2. Decoupled controllers.

In the system considered for the studies in this paper, the two generating units are connected to a load through two lines (modelled as π -sections). A simple RL load model is used to represent the load with connecting line resistances and inductances. The test system with two inverters is shown in Figure 3.

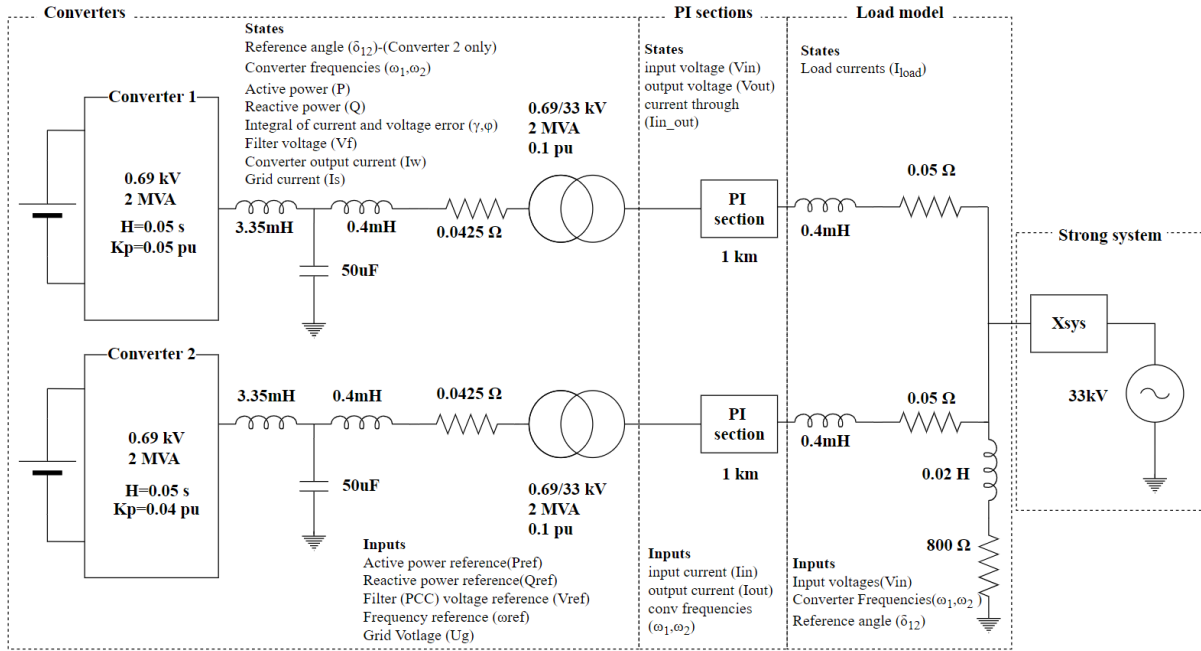


Figure 3. Overall system

3. MATHEMATICAL MODELLING OF THE TEST SYSTEM

3.1 Converter model

Mathematical models for grid-forming voltage controlled VSC converter systems with simple droop control are already presented in literature [6], [7]. This paper presents a model that extends these models by including the inertial control parameters in their power control loops.

The system was initially developed by connecting the converters to a strong system (infinite bus) through transformers and a LV lines. The DC side of the converter system is assumed to have an energy storage unit with fast dynamics that is not modelled for this study. It is important to note that the decoupled infinite bus voltages act as input of this system and that the output current towards the infinite bus is specified as a state of the system.

3.2 π -section and Load model

The converter is connected to the load through a π -section. The π -section acts as an interfacing element between the load model and the converter. Given that the terminal voltages at each end of the π -section are state variables, and the currents entering and leaving the π -section are inputs of the system, the π -section significantly reduces the mathematical complexity that arises when interfacing the load with the converter.

The load model is a common RL series load, which is fed through two short line segments. The line voltages at the sending end of the line are specified as the inputs of the state matrix while the currents at the sending end are states of the system.

3.4 Combination of models

The defined state-space models have input and state matrices that have interconnecting inputs and states, e.g., the converter model has the infinite bus voltage as input and output currents as states whilst the π -section has input voltages as states and incoming currents as inputs. These models are combined with each other by defining a set of input and output selection matrices for each model [10].

Decoupling the equations results in each converter being represented in its own reference frame. Hence it is required to set one source as the common reference frame and represent all the other sources with respect to this common reference frame [6]. In the two-unit system in this paper, the (dq) frame of the grid-forming converter 1 is used as the common reference frame. The total combined state space model consists of 43 states and 8 inputs.

4. STABILITY ANALYSIS

The stability analysis was conducted to analyse the system behaviour once the converters were disconnected from the strong system shown in Figure 3. The response of the controllers and the movement of eigenvalues were studied with the system operating in islanded mode.

Once the mathematical models are developed, the nonlinear equations of the model are solved to obtain an initial operating point of the system. The system parameters are shown in Figure 3. The obtained solutions are used to generate the eigenvalues of the linearized state space system. Perturbations are then given to the system inputs of the small signal models and the responses are compared with the responses generated in PSCAD/EMTDC to validate the accuracy of the model. A sample of the overlaid response traces is shown in Figure 4.

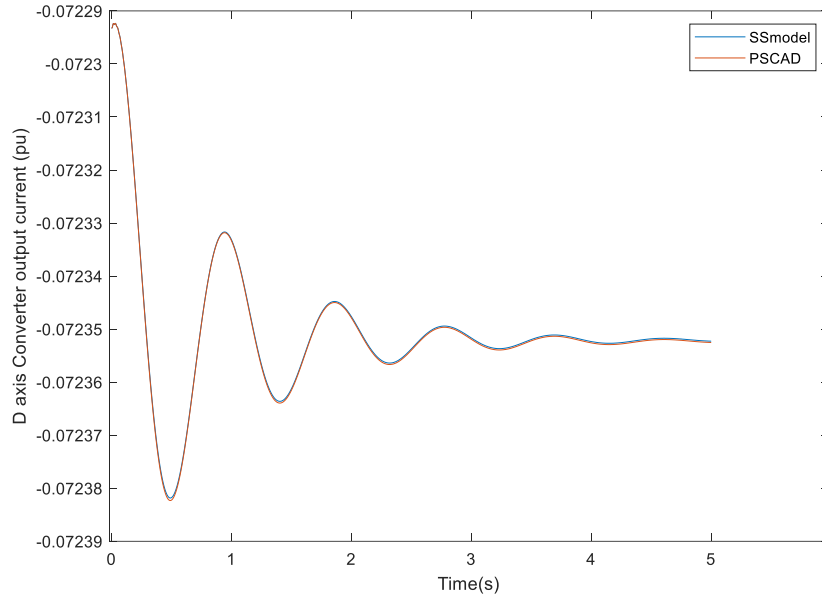


Figure 4. Variation of the inertia emulated converter output current for a 0.01 pu change in power reference ($H=5$ s, $K_p=0.04$).

4.1 Dual inverter with and without inertia emulation

The participation factors of the eigenvalues are calculated to identify the sensitivity of each eigenvalue to an associated state variable. The eigenvalues and their dominant states for the cases with and without inertia emulation are given in Table 1. The eigenvalues associated with the transmission line parameters and filter values are left out as they lie further away from the imaginary axis.

Table 1. Dominant modes and their associated states

With inertia emulation			Without inertia emulation		
No	Eigenvalues	Dominant states	No	Eigenvalue	Dominant states
1	-17.22±141.75	Converter output currents, frequency, and power angle between converters	1	-12.16±147.35	Converter output currents, power angle between converters
2	-612.8±150.93	Converter output currents	2	-616±134.97	Converter output currents
3	-1000±6.46 -1001±2.468	Active and reactive power	3	-983 -1009	Active and reactive power
4	-189.5 -243.5 -29.15 -13.67	Converter output frequency and power angle between converters	4	-25.53 -13.44 -18.55	Power angle between the two converters
5	-16.93±0.1032 -18.36 -13.67	Integral of error in decoupled voltage controller	5	-16.93±0.0999 -18.55 -13.44	Integral of error in decoupled voltage controller
6	-5.751±0.00197 -5.706 -5.841	Integral of error decoupled current controller	6	-5.751±0.0195 -5.706 -5.843	Integral of error in decoupled current controller

The eigenvalues in both converters are mostly identical except for the eigenvalue pairs 1 and 4. Eigenvalue pairs 1 and 2 depend on the LV line parameters and converter filter inductances. Compared with the non-inertia converter, the inertia emulating converter has additional damped eigenvalues in 4, located further away from the imaginary axis. All eigenvalues have a participation factor in the range of (0.1~1)

4.1.1 Eigenvalue sensitivity to active power droop gain

The movement of eigenvalues for a change in the active power droop gain is given in Figure 5. The droop gains are changed from 0.04 to 0.09 and the movement of the sensitive eigenvalues are shown. The system without inertia emulation shows that, as the droop coefficients are increased, the eigenvalue pair 1 moves towards the imaginary axis with an oscillatory frequency of 144 rad/s. Since eigenvalue pair 1 has high participation in converter output current, this oscillatory frequency varies with the change of converter filter inductance. In comparison, the corresponding eigenvalue pair for the inertia emulated converter move away from the imaginary axis. In both cases, one of the damped eigenvalues which has participation in converter output frequency and angle, shows movement away from the imaginary axis.

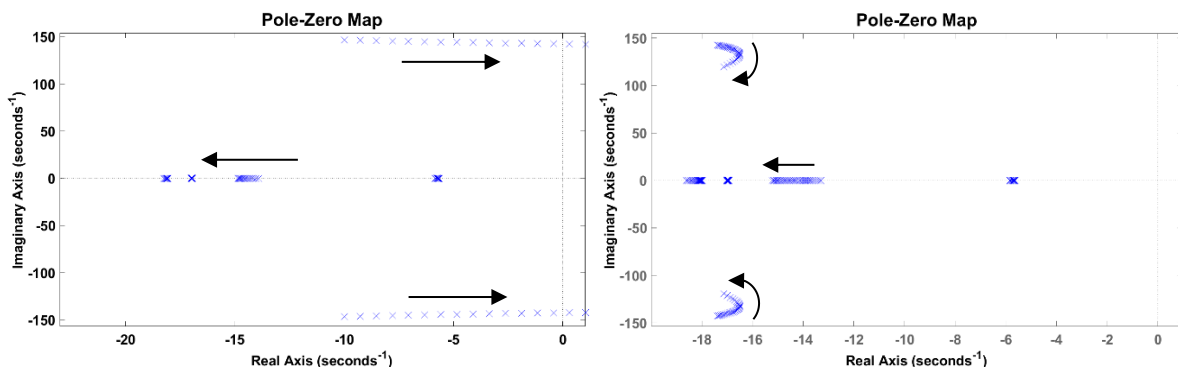


Figure 5. Eigenvalue trajectories without (left) and with inertia (right) emulation vs. droop

This behaviour can be explained using equation 2 of the inertia emulating converter. As opposed to the converter with static droop coefficient, the inertia emulating converter has a droop coefficient that is impacted by the dynamics of the system. During a power oscillation, the (T_{HS}/K_D+1) component acts as a low-pass filter damping out the frequency variations and creating a dynamic droop coefficient that is less than the static droop coefficient $1/K_D$ during transient conditions. This results in improved stability and allows a higher degree of freedom when selecting droop coefficients for the converter. On the contrary the non-inertia converter aggressively tries to control the system frequency as the droop coefficient is increased, leading the two converters to resolve to an unstable oscillatory state.

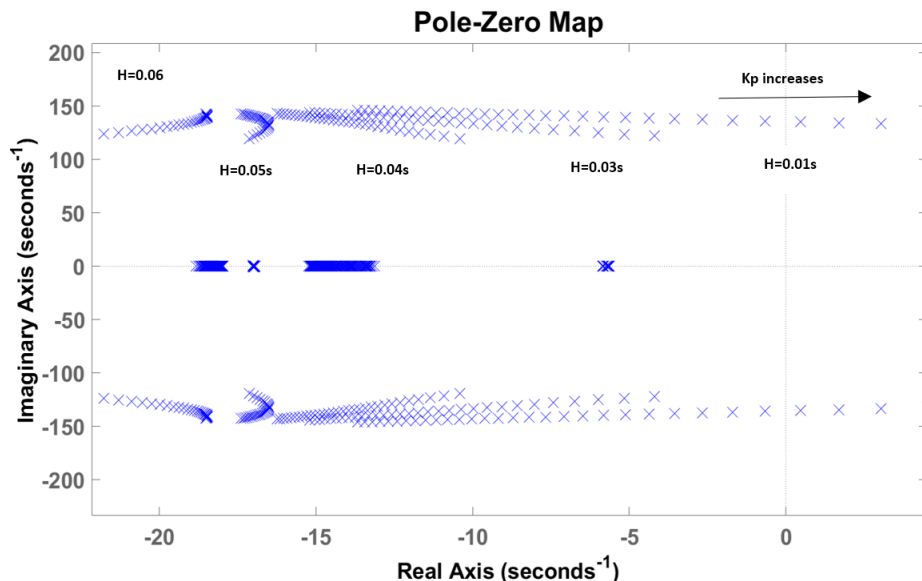


Figure 6. Movement of Eigenvalues with droop coefficient variation as inertia constant is increased

This is further demonstrated in Figure 6. The movement of eigenvalue pair 1 is shown with the increase of inertial constant from 0.01 to 0.06 s. It shows that as the inertial constant increases, the eigenvalue pair reduces its sensitivity to droop gain with slight reductions in frequency. For higher values of inertia, the eigenvalues can be seen moving away from the imaginary axis.

Since the eigenvalue pair 1 is sensitive to the converter output currents, increasing the LV line resistance shall also increase the damping and allow an increase for the active power gain in the converters without inertia emulation. A similar response for the same eigenvalues can be observed for a change in reactive power gain due to the coupling of active and reactive power in the LV lines. The movement is less compared to that of active power droop gain.

The EMT simulations results for the power measurements of the two converter arrangements are given in Figure 7. Once the droop coefficient is changed from 0.08 to 0.09, the active power measurements of the converter with simple droop controller show a gradually increasing oscillatory behaviour leading to instability. The oscillation frequency of can be found to be 23 Hz, which is equivalent to the imaginary component of the eigenvalue pair found in Figure 5. The power response measurement of the inertia emulated converter provides a stable response.

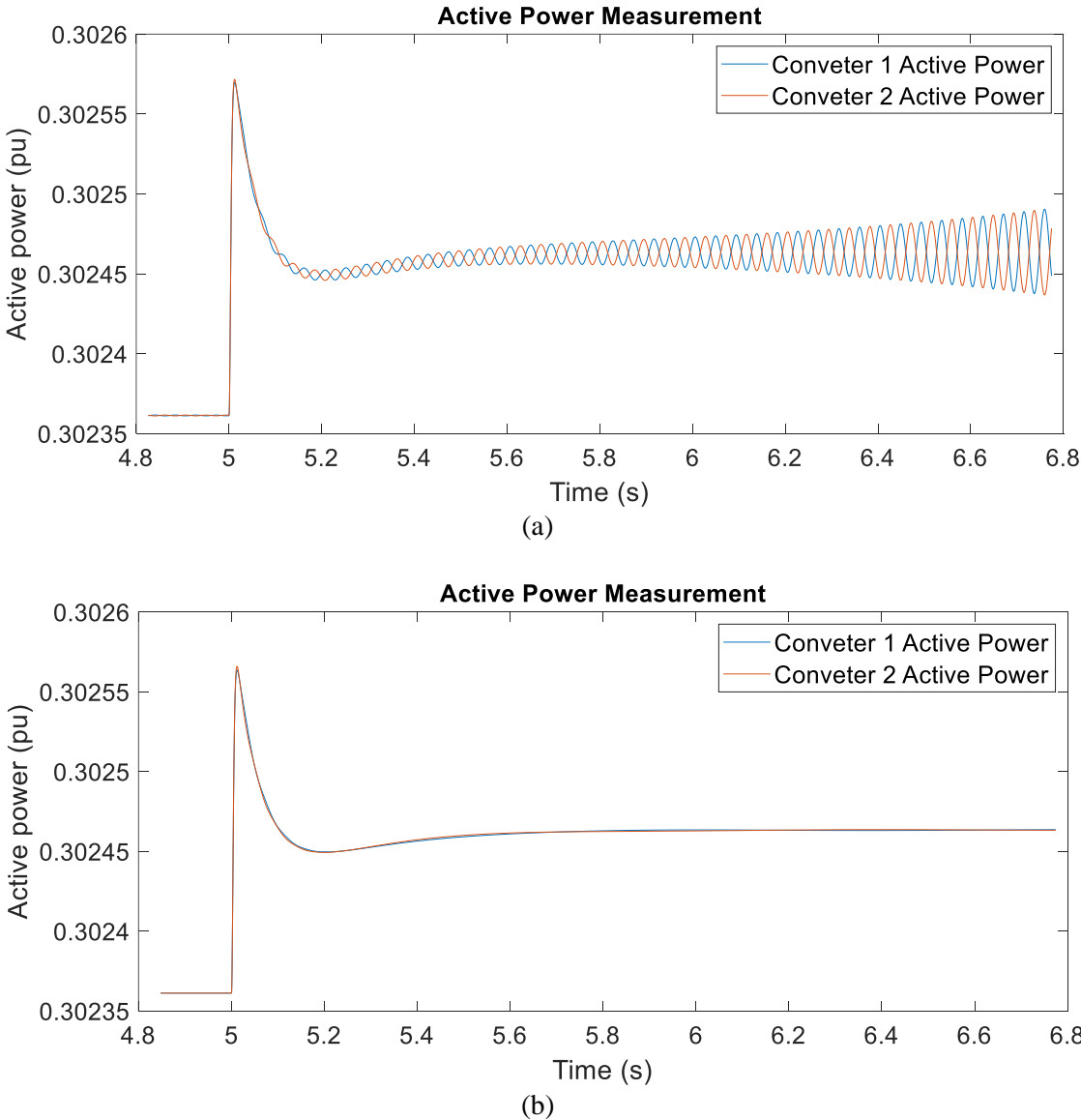


Figure 7. Power without (a) and with (b) inertial emulation (droop coefficient = 0.09).

4.1.2 Eigenvalue sensitivity to inertial parameters

The emulated inertial constant of the converter is varied from 0.05 s to 0.5 s to observe the movement of eigenvalues. The eigenvalues of 4 consist of damped eigenvalues that are sensitive to the converter frequency. As the inertial parameters are varied, the damped eigenvalues -29.1 and -189.5 move towards each other and form an oscillatory pair moving towards the origin. Given the oscillatory frequency (20-40 rad/s), these oscillations can be classified as inertial oscillations similar to those of synchronous machines.

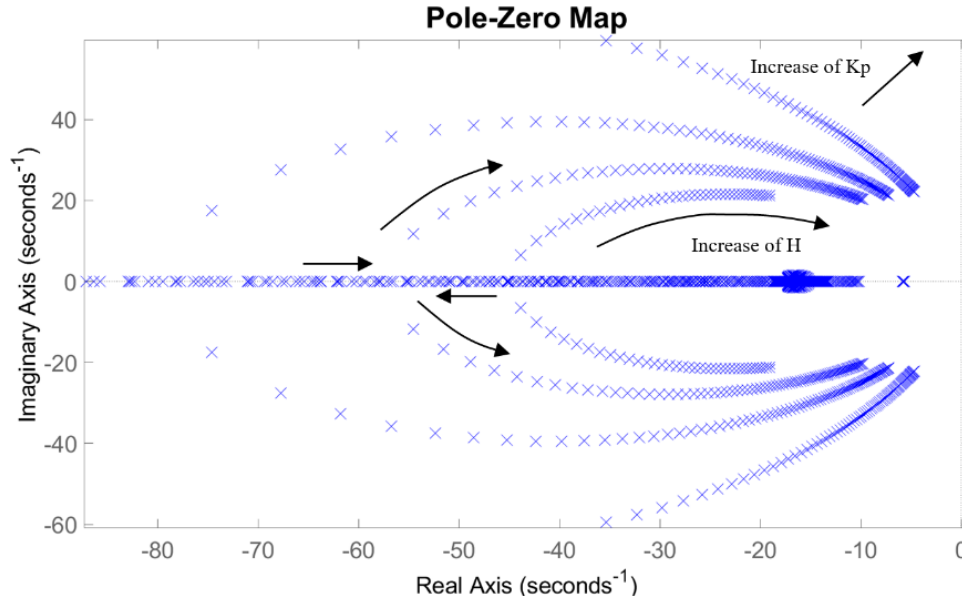


Figure 8. Movement of eigenvalues for a variation in emulated inertia from 0.05 s to 0.5 s, while varying active power droop coefficient from 0.04 to 0.1.

In order to explore the impact of droop coefficient on these trajectories, the eigenvalues were then observed while increasing the active power droop coefficients. As the droop coefficients increase the oscillatory frequency related to the inertial variations shows an increase. This can be explained using equation 2 and 3. Analogous to the synchronous machine, the droop coefficient of the converter becomes the reciprocal of the mechanical damping coefficient of the synchronous machine. Hence as the droop coefficient is increased, the inertial oscillations between the two converters shall experience reduced damping in their oscillations which results in the increased oscillatory trajectories as shown in Figure 8.

5. CONCLUSION

This paper presented a stability analysis for an inertia emulating grid-forming inverter system when it is islanded from a stable main grid. A comparison was presented between an inverter-based system with and without inertia emulation showing that the inertia emulating system is more stable when it comes to larger droop coefficients. The noninitial grid-forming converter tends to get unstable in this scenario.

The trajectories of eigenvalues of the inertia emulated converters were shown with the variation of the inertial parameter and its droop coefficients. It was shown that oscillation of the converter output power and frequency increases as the droop coefficient is increased. This was explained as the droop coefficient being the reciprocal of the equivalent mechanical damping coefficient of the generator swing equation model. These oscillations can be damped by utilizing additional control loops and utilizing the parameters of the DC side dynamics that generate the power reference input. This will be explored in future work.

BIBLIOGRAPHY

- [1] Q. Zhong and G. Weiss, "Synchronverters: Inverters That Mimic Synchronous Generators," *IEEE Transactions on Industrial Electronics*, vol. 58, no. 4, pp. 1259-1267, April 2011.
- [2] B. B. Johnson, S. V. Dhople, J. L. Cale, A. O. Hamadeh and P. T. Krein, "Oscillator-Based Inverter Control for Islanded Three-Phase Microgrids," *IEEE Journal of Photovoltaics*, vol. 4, no. 1, pp. 387-395, Jan. 2014.
- [3] B. B. Johnson, M. Sinha, N. G. Ainsworth, F. Dörfler and S. V. Dhople, "Synthesizing Virtual Oscillators to Control Islanded Inverters," *IEEE Transactions on Power Electronics*, vol. 31, no. 8, pp. 6002-6015, Aug. 2016.
- [4] J. Rocabert, A. Luna, F. Blaabjerg and P. Rodríguez, "Control of Power Converters in AC Microgrids," *IEEE Transactions on Power Electronics*, vol. 27, no. 11, pp. 4734-4749, Nov. 2012.
- [5] M. Mousavi, A. Mehrizi-Sani, D. Ramasubramanian and E. Farantatos, "Performance Evaluation of an Angle Droop—Based Power Sharing Algorithm for An Inverter-Dominated Power System," in *Proc. 2019 IEEE Power & Energy Society General Meeting (PESGM)*, Atlanta, GA, USA, 2019, pp. 1-5.
- [6] N. Pogaku, M. Prodanovic and T. C. Green, "Modeling, Analysis and Testing of Autonomous Operation of an Inverter-Based Microgrid," *IEEE Transactions on Power Electronics*, vol. 22, no. 2, pp. 613-625, March 2007.
- [7] S. Leitner, M. Yazdani, A. Mehrizi-Sani and A. Muetze, "Small-Signal Stability Analysis of an Inverter-Based Microgrid With Internal Model-Based Controllers," *IEEE Transactions on Smart Grid*, vol. 9, no. 5, pp. 5393-5402, Sept. 2018.
- [8] P. Kundur, *Power System Stability and Control*. McGraw-Hill, 1994
- [9] X. Hou, Y. Sun, X. Zhang, J. Lu, P. Wang and J. M. Guerrero, "Improvement of Frequency Regulation in VSG-Based AC Microgrid Via Adaptive Virtual Inertia," *IEEE Transactions on Power Electronics*, vol. 35, no. 2, pp. 1589-1602, Feb. 2020.
- [10] Eugene L. Duke, "Combining and Connecting Linear, Multi-Input, Multi-Output Subsystem Models", NASA Technical Memorandum, April 1986